

From chemisorption to mechanism on surfaces: An exploration of the pyrolysis of triisobutylaluminum in the chemical vapor deposition of aluminum thin films

A. W. Edith Chan and Roald Hoffmann

Citation: *J. Vac. Sci. Technol. A* **9**, 1569 (1991); doi: 10.1116/1.577663

View online: <http://dx.doi.org/10.1116/1.577663>

View Table of Contents: <http://avspublications.org/resource/1/JVTAD6/v9/i3>

Published by the AVS: Science & Technology of Materials, Interfaces, and Processing

Related Articles

Binding of styrene on silicon (111)-7×7 surfaces as a model molecular electronics system
J. Vac. Sci. Technol. A **30**, 031401 (2012)

Optimizing interfacial features to regulate neural progenitor cells using polyelectrolyte multilayers and brain derived neurotrophic factor
Biointerphases **6**, 189 (2011)

Patterning of alkanethiolate self-assembled monolayers by downstream microwave nitrogen plasma: Negative and positive resist behavior
J. Vac. Sci. Technol. B **27**, 1949 (2009)

Comment on "Survey on measurement of tangential momentum accommodation coefficient" [
J. Vac. Sci. Technol. A **26**, 634 (2008)
]

J. Vac. Sci. Technol. A **27**, 591 (2009)

Hydrogen mediated transport of Sn to Ru film surface
J. Vac. Sci. Technol. A **27**, 306 (2009)

Additional information on *J. Vac. Sci. Technol. A*

Journal Homepage: <http://avspublications.org/jvsta>

Journal Information: http://avspublications.org/jvsta/about/about_the_journal

Top downloads: http://avspublications.org/jvsta/top_20_most_downloaded

Information for Authors: http://avspublications.org/jvsta/authors/information_for_contributors

ADVERTISEMENT



Aluminum Valves with Conflat® Flanges

Less Outgassing Than Stainless
Mate to Stainless Steel Conflats
Sizes From 2.75 to 14 inch O.D.
Leak Rate Less Than 10^{-10} SCC/S

Visit us
at Booth # 300
in Tampa

Prices & Specifications
vacuumresearch.com



From chemisorption to mechanism on surfaces: An exploration of the pyrolysis of triisobutylaluminum in the chemical vapor deposition of aluminum thin films

A. W. Edith Chan and Roald Hoffmann^{a)}

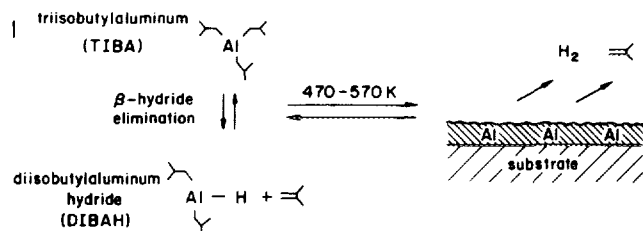
Department of Chemistry and Materials Science Center, Cornell University, Ithaca, New York 14853

(Received 17 August 1990; accepted 5 November 1990)

The chemisorption of H, CH₃, C₂H₅, and C₂H₄ is examined on Al(111) and Al(100) surfaces by the extended Hückel method, using a tight-binding formalism. A local chemical viewpoint is sought through fragment analyses, decompositions of the density of states and overlap populations. Various adsorption sites have been studied. On both surfaces, the first three species prefer to bind in the on-top site by a σ -type interaction with the coordinated Al atom. Ethylene, on the other hand, favors the twofold bridging site by a di- σ bonded interaction with its highest occupied molecular orbital and lowest unoccupied molecular orbital. In addition, the mobility of all these species on surfaces is investigated. Finally, the mechanism for the thermal decompositions of the triisobutylaluminum is studied. A β -hydride elimination rate-determining step is established, in which the activation barrier of the reaction in Al(111) is lower than Al(100). This result is in agreement with the experimental findings.

I. INTRODUCTION

How to grow pure, perfectly conforming thin films at low processing temperatures? Chemical vapor deposition (CVD) accomplishes this.¹ One aspect of this still growing field is aluminum CVD, in which the most extensively precursor used is triisobutylaluminum (TIBA). Aluminum CVD is used to form conductive contacts on silicon-based electronic devices. Back in the late 50's, Ziegler² and co-workers reported that TIBA can be pyrolyzed at ~ 520 K to deposit aluminum thin films. The overall process is reversible, and Ziegler suggested the potential of this system for refining Al. The microscopic mechanism by which the organic part of the TIBA precursor is shed on a surface is intriguing. One can use gas phase chemistry as a partial guide, the conversion of isobutyl ligands into isobutylene is one process that is observed. So is the formation of hydrogen, suggesting a β -hydride elimination mechanism. Above 470 K, TIBA mainly decomposes on Al surfaces to deposit Al and evolve isobutylene and H₂. This is shown in diagram 1 below:

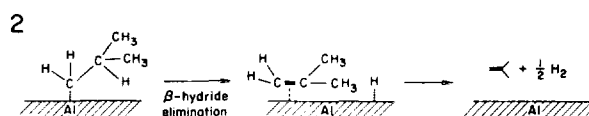


Bent, Nuzzo and Dubois³ have investigated this system thoroughly. Their kinetic studies confirmed that the reaction mechanism involves a β -hydride elimination, which is also the rate determining step. Interestingly, these researchers reported that the reaction is two to five times faster on Al(111) than Al(100). The measured activation energy is 1.2 and 1.4 eV (28 and 33 kcal/mol) for Al(111) and Al(100), respectively.

Higashi, Raghavachari, and Steigerwald,⁴ using *ab initio* quantum chemical techniques, investigated the mechanism of surface selectivity of this process with a molecular model, a planar H₂AlCH₂CH₃. They concluded that in the β elimination, the Al atom, having a tetrahedral configuration in the transition state, is using its empty out-of-plane $p\pi$ orbital to help lower the activation barrier. Their calculated activation energy (which is thus related to the sigma to empty p electron excitation) is 1.2 eV. In spite of the importance of these types of systems, very little experimental data on molecules adsorbed on Al exist.

In this paper, we explore possible mechanisms for the reaction of TIBA on surfaces. To do this, we utilize tight-binding extended Hückel calculations, and the tools of density of states (DOS), including local or projected DOS contributions, crystal orbital overlap populations (COOP), and overlap populations (OP).⁵ A fragment analysis allows us to compare the changes between the bare surfaces, the adsorbates, and the composite chemisorbed system. Please refer to the Appendix for further computational information.

The later stages of the mechanism proposed by Bent *et al.*³ are sketched in diagram 2:



First TIBA is deposited on the surface. Then it is suggested that the isobutyl ligands diffuse readily across the surface, independent of the Al atom to which they were originally attached. This is also observed in solution, where alkyl ligands readily exchange between terminal and bridging positions in dimeric aluminum alkyls.⁶ The critical β elimination forms adsorbed isobutene and H atoms on the surface, which in turn eventually desorb as H₂ and isobutene.

We begin our studies by replacing the two methyl groups

not directly involved in the reaction by hydrogens. Thus, instead of an isopropyl group we investigate an ethyl, CH_2CH_3 . We proceed to examine the chemisorption and migration patterns of CH_2 , CH_3 , ethylene, and H on various Al surfaces, supplementing these by an investigation of the binding of CH_3 . Following these preliminaries we calculate a potential energy surface for the β elimination reaction.

II. METAL SURFACES

One simple way to model a metal surface is by a finite slab.⁷ The question arises as to how many layers are required to simulate reliably the properties of the surface and the bulk. The choice of the thickness of the slab could be justified by comparing the net charges and also the metal-metal overlap populations with those of the bulk Al. Therefore, first of all, we present some properties of bulk Al and then proceed to the surfaces.

Al metal has a face-centered-cubic (fcc) structure,⁸ with nearest neighbor distance of 2.86 Å. Al is a high-density, nearly free electron metal. Its bands, which are a mixture of *s* and *p* orbitals, are very dispersive. The extended Hückel method's valence state ionization potentials for the Al atom are obtained by charge iteration.⁹ They are -12.6 and -7.0 eV for the *s* and *p* orbitals, respectively. The DOS [Fig. 1(a)], of course, does not have a characteristic *d* peak, as the transition metals do.⁷ The projected *s* states in Fig. 1(a) indeed are very dispersive. 60% of the *s* orbitals are filled, as measured by the integration curve (dotted line) for the projected DOS up to the Fermi energy, while only 30% of the *p* orbitals are occupied. The Al-Al COOP [Fig. 1(b)] curve indicates that Fermi level is very near the turning point of the Al-Al metal bond strength. All the states below ϵ_f are Al-Al bonding, while strong Al-Al antibonding occurs above it. In other words, three electrons per atom is the opti-

mal count, in terms of cohesive energy, for Al metal. The computed Fermi energy is -6.12 eV and the Al-Al OP is 0.206.

The Al(111) plane is a hexagonal surface while the Al(100) plane is a square one. Table I lists some calculated indices for the two surfaces. We studied 3 to 6 layer slabs and found reasonable convergence at 4 layers. The DOS and COOP curves of the Al(100) surface model are also shown in the right panels of Fig. 1. Those for Al(111) do not appear that different in their gross features.

Experimental studies, e.g., ultraviolet photoelectron spectroscopy (UPS), and high-resolution electron energy-loss spectroscopy (HREELS), have been done on Al surfaces. The typical HREELS spectra exhibit a very flat and structureless spectrum, typical of an Al *s*, *p* band.^{10,11} On the other hand, photoemission spectra^{12,13} have various peaks 2 to 3 eV below ϵ_f on a sloping background for both surfaces. These transitions are due to surface states.

The Al-Al OPs in the surface model are not that different from the bulk, as Table I shows. The surface Al-Al OP of Al(100) is bigger than that of Al(111) (0.32 versus 0.24). There are nine and eight nearest neighbors for Al(111) and Al(100), respectively. On Al(100), the Al atoms on the surface are more tightly bonded with each other due to fewer nearest neighbors. Therefore, the surface metal-metal bond is stronger on Al(100). In addition, the Fermi energy of Al(111) is about 1 eV higher than that of Al(100). More charge transfer to acceptor adsorbates is expected on Al(111).

The electron configuration of the surface Al atom is $s^{1.07}p^{2.07}$ and $s^{1.24}p^{2.16}$ for Al(111) and Al(100), respectively. The surface of Al(100) thus appears to be more electron rich than that of the (111) face. Below the Fermi level, the percentages of the occupation of the surface states are as follows: Al(111)-55% *s*, 42% *p_z*, and 31% *p_x* and *p_y*, Al(100)-62% *s*, 45% *p_z*, and 31% *p_x* and *p_y*. Most of the *p_x*

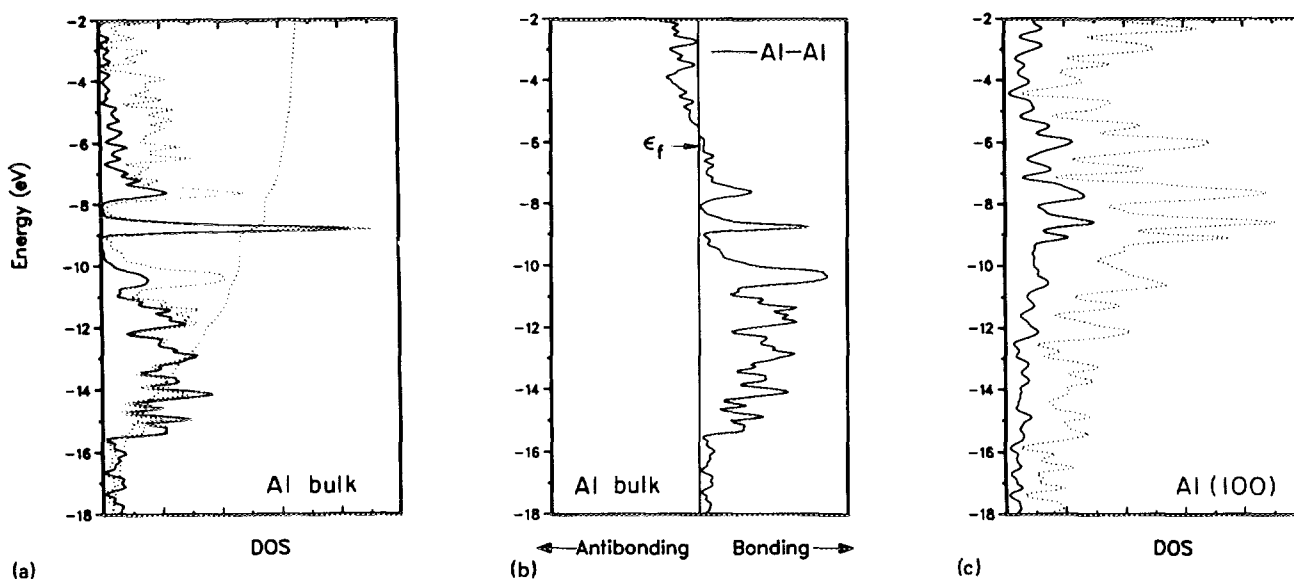


FIG. 1. (a) DOS of Al bulk metal, with projected *s* states (2x) and its integration curve (dotted line). (b) Al-Al COOP curve of the bulk Al metal. (c) DOS of clean Al(100), with projected surface states (solid line).

TABLE I. Calculated results for a four layer slab of Al(111) and Al(100).^a

	Al(111)	Al(100)
Electron densities		
Surface—total	3.14	3.40
Surface— <i>s</i>	1.07	1.24
Surface— <i>p</i>	2.07	2.16
Bulk—total	2.86	2.60
Bulk— <i>s</i>	1.06	1.02
Bulk— <i>p</i>	1.80	1.58
Overlap populations		
On surface	0.24	0.32
Surface—bulk	0.24	0.21
Inside slab	0.21	0.20
ϵ_f (eV)	-5.45	-6.43

^a Al bulk: $\epsilon_f = -6.12$ eV, Al-Al OP = 0.21.

and p_y states are above the Fermi energy. Their match in energy with adsorbate levels is poor since the ϵ_f is so high.

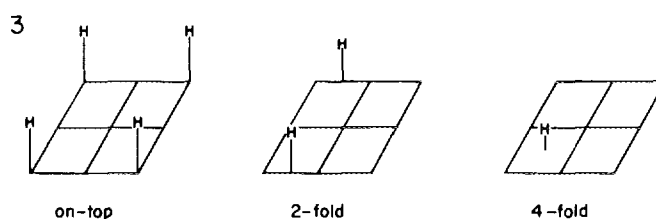
III. ATOMIC HYDROGEN

A fairly complete picture of the geometry of the atomic H-surface bond has been obtained during the last decade,¹⁴ primarily based on dynamical low-energy electron diffraction (LEED)¹⁵ structure analyses, or HREELS¹⁶ measurements. The hydrogen usually occupies a multicenter coordination site on transition metal surfaces, such as the threefold or fourfold site.¹⁴ The H-metal bond length ranges from 1.72 to 1.91 Å for transition metals.¹⁴ Electron energy-loss spectroscopy (EELS) and thermal desorption spectroscopy (TDS) studies¹⁷ of hydrogen adsorption on Al(100) show that H adsorbs on the bridging site at $T < 90$ K, while at 150 K, it is also terminally coordinated.

Hjelmberg, using the Kohn-Sham scheme within the framework of a jellium model, has done calculations on H chemisorption on Al surfaces.¹⁸ He predicted that H adsorbs on the bridge site on Al(100), on-top or bridge site on Al(111), with Al-H distances of 1.78, 1.53, and 1.78 Å, respectively. On the other hand, Smirnov,¹⁹ using complete neglect of differential overlap (CNDO) calculations within a cluster model, predicted that H adsorbed on the fourfold site, with a distance of 2.13 Å. The other distances their calculation found, for on-top and twofold sites, were 1.61 and 1.82 Å, respectively. Xie and Schaefer²⁰ predicted the Al-H distances are between 1.55–1.56 Å for $\text{HAl}(\text{C}_x\text{H}_x)$ complexes in an *ab initio* quantum mechanical study. We think it is safe to take the H-Al bond length from that of a discrete molecule. In AlH_4^- and H_3AlNCH_3 ,²¹ it is 1.55 and 1.56 Å, respectively. We will use 1.55 Å for the on-top and twofold sites. On the threefold and fourfold sites, hydrogen is put right in the plane of the surface, which makes the Al-H distance 1.653 (threefold) and 2.00 Å (fourfold), respectively. The Al-H OP this method calculates for AlH_4^- is 0.636. This will be a reference point for studying the Al-H OP on the surfaces.

We proceed to the study of H on the two Al surfaces. To ensure minimal interaction between adsorbates, a $p(2 \times 2)$ unit cell is chosen on both surfaces, corresponding to adsor-

bate coverage of 1/4. On-top twofold, threefold (fcc site) sites will be considered for the (111) surface, along with on-top, twofold, fourfold sites for the (100) surface. These are illustrated for the example of chemisorbed H on Al(100) in diagram 3:

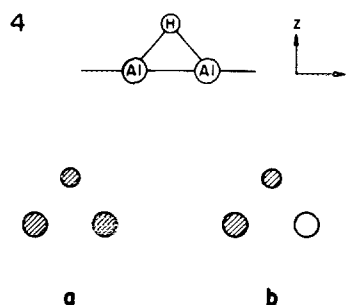


Our investigations focus on two bonding criteria: binding energy (BE) and overlap populations. A positive binding energy means a stabilizing interaction has taken place between the adsorbate and the surface. The crucial BE and OPs calculated are compiled in Table II for different sites. The BE are all positive, indicating a stabilizing interaction between H and the surfaces. This is largest for the on-top site, and smallest for the three and fourfold sites.

It is difficult to correlate the overlap population with bond order (or bond strength) directly, but if we assume that the Al-H in AlH_4^- is a single bond (OP = 0.637), then there forms one strong bond in the on-top site, two somewhat weaker bonds in the twofold site and three (or four) still weaker bonds in the three or fourfold site. Following mainly the BE, we think the adsorption site likely to be favored is the on-top site.

As mentioned before, H adsorbs on transition metals primarily in higher coordination sites. The differences in preferred adsorption sites between Al and transition metals are understandable. Transition metals may drive the H to a higher local coordination site, due to the potentialities of overlap with their *d* orbitals.²² However, on the Al surface, the $s + p_z$ hybrid orbitals will have a bigger overlap with the hydrogen *s* orbitals in the on-top site. As one can move from the onfold on top to a higher coordinated site, the $\langle \text{Al}(s + p_z) | \text{H}(s) \rangle$ decreases while $\langle \text{Al}(p_x + p_y) | \text{H}(s) \rangle$ increases.

Let us discuss each orbital in detail. In the on-top site, by reason of symmetry, the H 1s orbital can interact with the whole Al *s* band, while in the twofold or threefold site, it can only interact with the orbitals near the bottom of the bands, type diagram 4(a), but not diagram 4(b):



The case for Al p_z bands is simpler. The OPs (see Table II) are directly related to the overlap. The zero value for the $\text{Al}(p_z)\text{-H}(s)$ OP in the three and fourfold sites is due to the

TABLE II. Calculated results for the adsorption of H.

	On top		Twofold		Threefold/fourfold	
	111	100	111	100	111	
100						
BE (eV)	7.709	5.200	3.931	3.786	2.550	
0.247						
Overlap populations						
Al-Al ^a	0.243	0.283	-0.018	-0.067	0.020	0.258
Al ^b -H	0.607	0.606	0.411	0.405	0.261	0.120
Al s-Hs	0.227	0.184	0.121	0.108	0.074	-0.012
Al p _x -Hs	0.000	0.000	0.097	0.133	0.187	0.067
Al p _y -Hs	0.380	0.421	0.110	0.096	0.000	0.000
Net charge						
H	-0.517	-0.459	-0.427	-0.362	-0.281	
-0.298						
Al ^b	+0.275	+0.216	+0.198	+0.026	+0.160	
...						
Al ^c	-0.186	-0.500	-0.226	-0.477	-0.243	
-0.230						

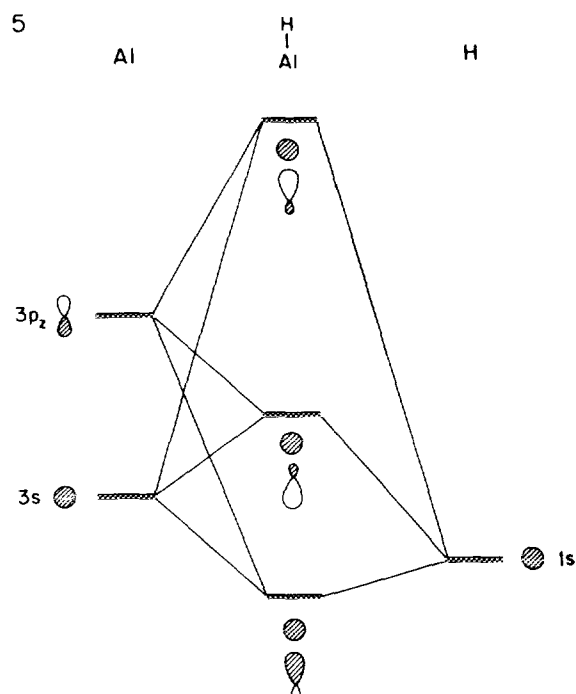
^aSurface Al-Al bond.^bSurface Al directly coordinated with H.^cSurface Al not coordinated with H.

H lying in the plane of the surface in these geometries. What about Al $p_x + p_y$ orbitals? Those lie higher in energy, so the match between them and H 1s is quite poor. Even though their overlaps are substantial, few such states are occupied, and so their contribution to the Al-H OP is small.

Another interesting feature is the surface Al-Al overlap population. The Al-Al metal surface bond is considerably weakened on going from on-top H coordination to threefold. This bond weakening is a direct consequence of a stronger Al-H interaction, which pushes some Al-Al bonding states up above the Fermi level. The more strongly the Al and H interact, the more Al-Al states will be pushed up, which then results in a weaker surface metal-metal bond. Actually H adsorbed in an on-top site is not that uncommon, it occurs on semiconductor surfaces.¹⁴

In the remainder of this section, we discuss the binding characteristics of the on-top site in detail. Figure 2 shows the Al-H COOP curves and DOS, with H contributions to each surface. The bar on the right in the DOS plot indicates the energy level of H 1s orbital before interaction. This orbital is stabilized after adsorption, and 25% of its states are pushed up above the Fermi level.

The orbital effects for both surfaces are similar. Diagram 5 illustrates the essence of this interaction in a local three-orbital model. The lowest and highest levels are bonding and antibonding among all three orbitals while the middle one is bonding between H 1s and Al p_z but antibonding between H 1s and Al s. In the COOP curves the region below -13 eV corresponds to the lowest level in diagram 5, above that to the middle level. There is more Al-H antibonding above the window of this graph.



Finally, the electron transfer from metal to H is bigger on Al(111) than Al(100), by about 0.06 e^- (both in the on-top and twofold hydrogen sites), as we expected. H chemisorption on Al metal occurs through a σ type interaction, involving essentially surface $s + p_z$ orbitals. As H moves along this series of geometries, from on top to 3/4-fold sites, more Al-H bonds are formed. But these are individually weaker, and

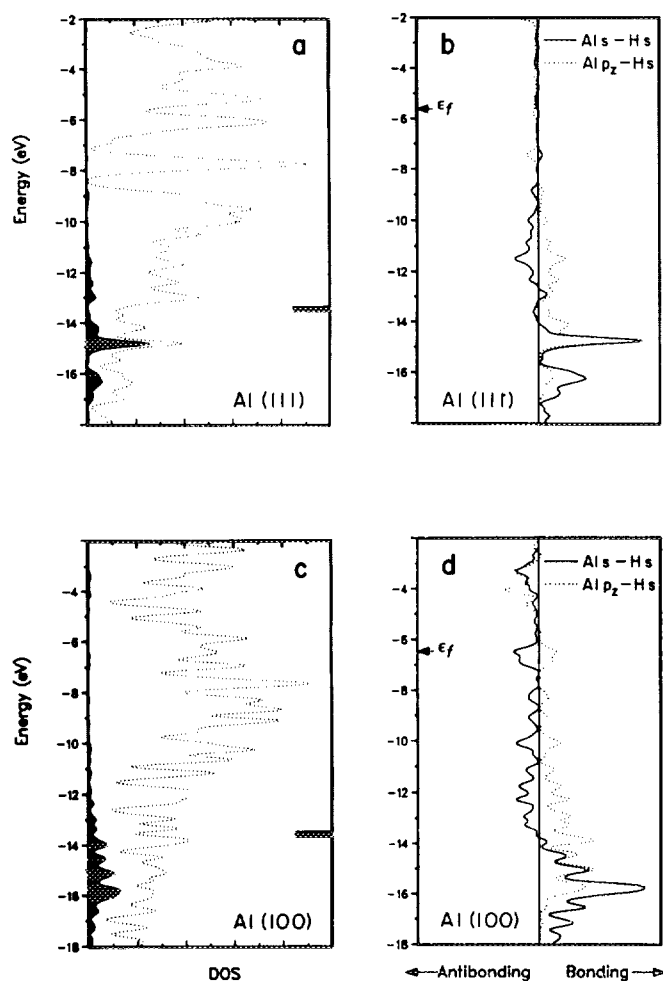


FIG. 2. (a) DOS of H adsorbed in the on-top site on Al(111), with projected DOS of H (2x) and its integration curve (dotted line). The bar indicates the H 1s energy before adsorption. (b) Al-H COOP curves in an atomic basis in the on-top site on Al(111). (c) DOS of H adsorbed in the on-top site on Al(100), with projected DOS of H (2x) and its integration curve (dotted line). The bar indicates the H 1s energy before adsorption. (d) Al-H COOP curves in an atomic basis in the on-top site on Al(100).

Al-H bonding is achieved at the expense of weakening of Al-Al surface bonds. As a result, the chemisorption favors the on-top position.

IV. CH₃ ON Al SURFACE

In a gas phase electron diffraction investigation²³ of Al(CH₃)₃, the bond distances found for C-H and Al-C were 1.11 and 1.96 Å, respectively. The Al-C-H angle is 120°. For organometallic Al compounds, the Al-C distance ranges from 1.9 to 2.4 Å.²³⁻²⁵ In this paper, the Al-C distance is fixed as 2.2 Å for all the C adsorbates, throughout the calculations. The HCH angle is kept as 110°. The Al-C OP calculated for Al(CH₃)₃ is 0.56 at Al-C 1.96 Å. At 2.2 Å, the Al-C OP is 0.49. This value, approximating a Al-C single bond, will serve as a reference point when comparing the Al-C OPs on surfaces. Our group has studied C₁ fragments on various transition metal surfaces in previous work.²⁶ We calculated that CH₃ should adsorb in the on-top site of the surfaces, however, other calculations²⁷ and some experimental results²⁸ are indicative of different bonding modes on transition metals.²⁹

A summary of the calculations is given in Table III. Judging by the binding energy, the Al-C and surface Al-Al OP, CH₃ chemisorption is very similar to that of H. In both cases the on-top site favored.

The Al-C overlap populations of all three surfaces differ a lot. In the on-top site, there is a strong Al-C bond. There are two weaker bonds on the twofold site and 3 (4) even weaker bonds on the threefold (fourfold) site. The surface metal-metal interaction also has a profound influence on the stabilization of the whole system. The more Al-C bonds are formed, the weaker the surface Al-Al bonds become. The reason for this is the same as in the hydrogen case: the Al-C bond is formed at the expense of weakening of the surface Al-Al bonds.

Since the behavior of both surfaces is similar, we will use Al(111) to illustrate the chemisorption in the on-top site. The half-filled highest occupied molecular orbital (HOMO)

TABLE III. Calculated results for the adsorption of CH₃.

	On top		Twofold		Threefold/fourfold	
	111	100	111	100	111	100
BE(eV)	4.543	2.734	0.433	-0.512	-1.430	-8.856
Overlap populations						
Al-Al	0.249	0.292	0.068	0.073	0.041	0.096
Al-C	0.426	0.429	0.225	0.222	0.144	0.080
Al s-n	0.154	0.124	0.083	0.078	0.056	0.023
Al p _x -n	0.000	0.000	0.063	0.075	0.054	0.023
Al p _z -n	0.279	0.315	0.089	0.086	0.036	-0.011
Electron occupations						
n	1.643	1.584	1.625	1.579	1.618	1.773
Net charge on CH ₃						
	-0.632	-0.566	-0.503	-0.481	-0.406	-0.448

(n) of the CH_3 fragment is drawn in 6, its energy in the free molecule is -11.77 eV. It consists of 95% $\text{C } p_z$ and 2% of $\text{C } s$. After adsorption, this fragment molecular orbital (MO) is spread out, mainly between -14 to -9 eV [Fig. 3(a)]. About 15% of these n CH_3 states are pushed up above the Fermi level.



Since the HOMO is a σ -type orbital, it interacts most efficiently with the Al $s + p_z$ orbitals. The Al($s + p_z$)- CH_3 (HOMO) OP is 0.433, which is 101% of the total Al-C OP. Figure 3(b) shows the COOP curves between the Al($s + p_z$) and CH_3 (HOMO). The bars indicate the energy level of the Al atomic component orbital and the position of the HOMO. We can interpret these COOP curves by a three level interaction again. Below -12 eV one has bonding between Al($s + p_z$) and the HOMO, above -6 eV is their antibonding counterpart, in the middle is bonding between Al p_z and the HOMO but antibonding between Al s and the HOMO.

The n band is more than half populated, with $1.64 e^-$ in it. The net charge on the methyl group is -0.63 . This brings the CH_3 closer to a CH_3^- upon adsorption. Again there is about $0.06 e^-$ more transferred from Al(111) to the molecule than from the Al(100) surface.

One may expect the π -type interaction is quite important in the twofold or threefold site. The methyl π or π^* type orbitals (made up of σ and σ^* CH orbitals) would interact with the p_x and p_y bands of the Al. However, the methyl π is located at around -14 eV, far from the Al p_x and p_y states. π^* , on the other hand, lies at 4 eV. There it matches in energy the Al p_x and p_y , but there is almost no stabilization arising

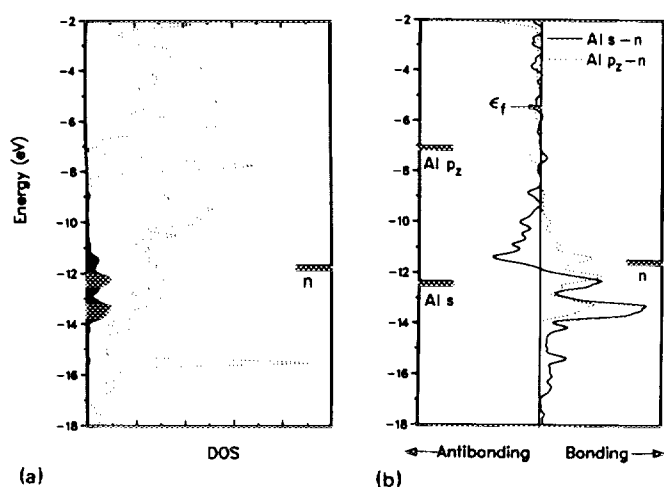


FIG. 3. (a) DOS of CH_3 adsorbed in the on-top site on Al(111), with projected DOS of the HOMO ($2\times$) and the integration curve (dotted line). The bar indicates its energy before adsorption. (b) Al-C COOP curves in an atomic basis in the on-top site on Al(111). The bars at left represent the atomic energies of Al $3s$ and $3p$. The bar at right denotes the energy of the HOMO of a free CH_3 .

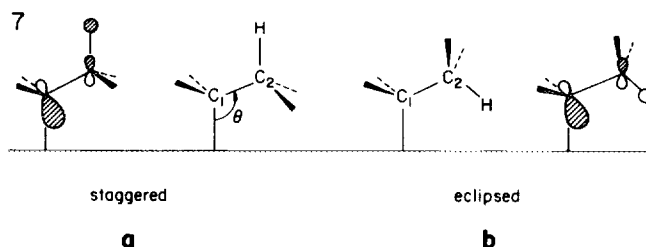
J. Vac. Sci. Technol. A, Vol. 9, No. 3, May/June 1991

from the interaction of these empty orbitals. The Al-C(π) and Al-C(π^*) OPs are very small in the twofold site: 0.007 and 0.015, respectively.

The bonding interaction between CH_3 and Al metal is similar to that of hydrogen, both H and CH_3 are predominantly engaged in σ -type interaction with the surface $s + p_z$ bands.

V. THE REACTANT— C_2H_5 RADICAL

C_2H_5 is isolobal with CH_3 . The interactions of ethyl should be quite similar to those of CH_3 . The big lobe of the half-filled HOMO, diagram 7, of CH_3CH_2 is localized on C_1 and is at -11.57 eV.



Xie and Schaefer, in their *ab initio* study, predicted that the global minimum of an Al C_2H_5 complex resembles the structure of diagram 7(a), with C-C distance = 1.54 Å and Al-C-C angle = 115° .²⁰ In this study, the C-C distance is kept at its single bond length, 1.54 Å, with the H-C-H angle at 110° . The staggered geometry (around the C-C bond) is more stable than the eclipsed one by about 0.15 and 0.18 eV on the Al(111) and Al(100) surfaces, respectively. Some repulsion between the methyl group and the surface is expected. The staggered configuration is then used for the adsorption geometry. The angle θ , defined as indicated in diagram 7, will be optimized. Threefold and fourfold sites will not be considered, because of the unfavorable binding energy calculated for these in the case of the CH_3 fragment. Only on-top and twofold sites will be studied. The results of the calculations are presented in Table IV.

From the binding energy, Al-C and Al-Al surface OP, the on-top site is the most favored one, as in the methyl case. We will discuss the Al(111) interaction in detail, as before. The bar on the right in the DOS plot in Fig. 4(a) shows the position of the HOMO (the ethyl radical lobe) before interaction. It is stabilized by about 0.3 eV after the interaction. From the Al-C COOP curve in Fig. 4, its main contribution is from the combination Al($s + p_z$)- CH_3CH_2 (HOMO). The HOMO, which has this lobe pointing directly towards the surface, achieves maximum overlap with the $s + p_z$ bands. In the COOP curves, a three-level interaction pattern is seen again between Al $s + p_z$ and the n orbital.

The C-C overlap population for the on-top site is around 0.74, which is the same as the gas phase C-C OP calculated for ethyl by the extended Hückel method. After chemisorption, the C-C bond is not weakened at all. In the twofold site, this OP is 0.04 smaller. This is due to a weak interaction of both carbons with the surface Al atoms.

The net charge for C_2H_5 is -0.6 (on-top site), which makes the ethyl group similar to a C_2H_5^- , just as in the CH_3

TABLE IV. Calculated results for C_2H_4 chemisorption.

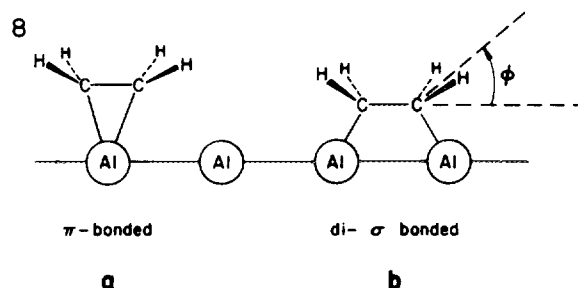
	On top		Twofold	
	111	100	111	100
θ	125°	125°	135°	140°
BE(eV)	3.937	2.098	-0.402	-1.259
Overlap populations				
C-C	0.739	0.736	0.696	0.692
Al-C	0.450	0.452	0.269	0.266
Al-n	0.440	0.445	0.142	0.140
Al s-n	0.156	0.126	0.050	0.052
Al p_x -n	0.000	0.000	0.039	0.044
Al p_z -n	0.284	0.318	0.053	0.044
Electron occupations				
n	1.644	1.586	1.618	1.577
Net charge on C_2H_4				
	-0.616	-0.554	-0.477	-0.454

case. There is about 0.06 more electron charge transfer from Al(111) to the adsorbate. The interaction of C_2H_4 is through the HOMO and the Al $s + p_z$ orbitals.

VI. C_2H_4 ON SURFACES

Al-ethylene complexes have been a subject of much interest.³⁰ The analysis of electron spin resonance (ESR) spectra showed that the Al atom-ethylene complex is formed through dative bonding, from the interaction of the π orbitals of the olefin and the valence orbitals of the Al atom.³⁰ This π -bonded structure, which is drawn in diagram 8(a), resembles a C_2H_4 chemisorbed in the on-top site on a surface. Schaefer *et al.*³¹ have done a detailed *ab initio* calculation on the Al-ethylene complex. The Al-C and C-C bond distances they calculate for the most stable ground state con-

figuration, 2B_2 [drawn in diagram 8(a)] is 2.228 and 1.417 Å, respectively. Gao and Karplus³² obtained similar results (also a 2B_2 ground state) in another *ab initio* study, with Al-C and C-C distances of 2.256 and 1.408 Å, respectively.



For most transition metals, two types of ethylene adsorption are detected on surfaces.³³ They have been assigned to a π -bonded [8(a)] species³⁴ and a di- σ bonded diagram [8(b)] alternative.³⁵ Both photoemission³⁶ and HREELS³⁷ studies have shown that ethylene upon chemisorption undergoes out-of-plane bending and some carbon-carbon bond weakening.

In our calculation, Al-C and C-C are fixed at 2.2 and 1.45 Å, respectively. The bending angle ϕ which is defined in diagram 8, is then optimized. This angle actually controls how much the s and p_x orbitals mix into the p_z orbitals in ethylene π and π^* , and therefore, how "bent" the lobes pointing towards the surface (or away from each other) are when C-C is stretched. This angle may also depend on the C-C distance. So, to optimize ϕ is indirectly to optimize the overlap between the lobes of the adsorbate and the symmetry related orbitals of Al on the surface. The results for different sites are very similar: the optimum ϕ is 45° for the on-top site, 50° for the two-fold site, and 50° for the 3/4-fold site on both surfaces.

Diagram 9 depicts the frontier orbitals which are expected to have the most interaction with the metal surface. Aside from the familiar (but now hybridized) π and π^* , we include the highest lying σ orbital as well. Note its lobes point "toward" each other.

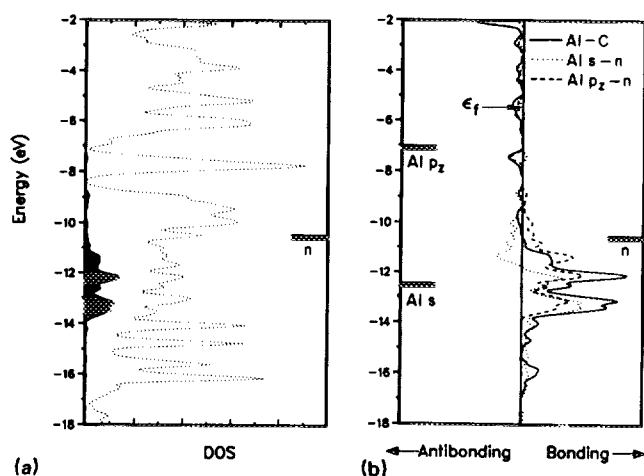


FIG. 4. (a) DOS of C_2H_4 adsorbed in the on-top site on Al(111), with projected DOS of the HOMO ($2\times$) and the integration curve (dotted line). The bar indicates its energy before adsorption. (b) Al-C COOP in a FMO basis in the on-top site on Al(111). The bars at left represent the atomic energies of Al $3s$ and $3p$. The bar at right denotes the energy of the HOMO of a free C_2H_4 .

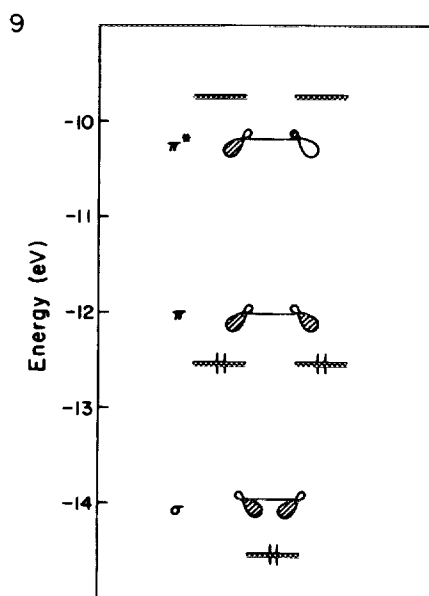
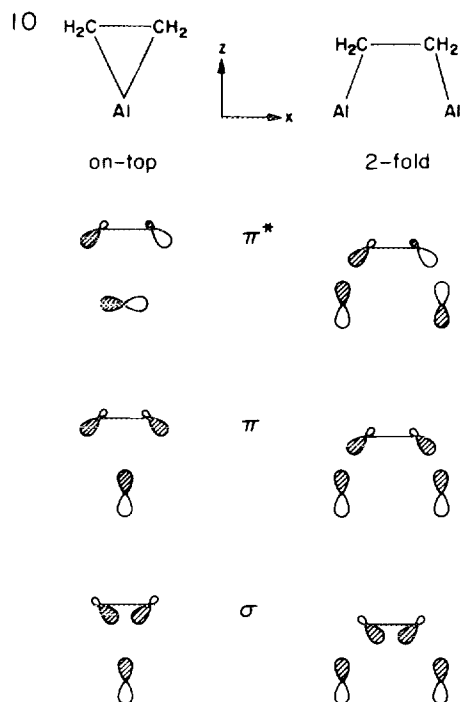


Table V lists the binding energies, overlap populations and electron occupations for the fragment molecular orbitals (FMOs) for different sites. Comparing BEs, threefold and fourfold sites are judged to be not very favorable for the chemisorption. The values of Al-C OP indicate that the Al-C bond strength is comparable to that calculated for CH_3 or C_2H_5 . The Al-C OP is the biggest on the twofold site. There are then two strong Al-C bonds formed, one weaker Al-C in the on-top site and 3/4 even weaker bonds in the 3/4-fold site. So just from the simple BE and Al-C OP arguments, we conclude that ethylene is likely to adsorb as a di- σ bonded species in the twofold site.

Since both surfaces behave similarly, we use Al(100) as an example. Figure 5 decomposes the Al-C OP into an Al- C_2H_4 FMO basis for the on-top and twofold sites. Both of these plots are on the same scale, so one can actually compare the area of each peak.

Looking at the schematic representation in diagram 10, the σ orbital should have a bigger overlap with the Al atom in the on-top site than the twofold site. Since σ is quite low lying (-14.54 eV), the Al- σ antibonding states after interaction are pushed up to around -13.8 eV. Therefore, there is no net gain in Al- σ bonding because of filling of both the bonding and the antibonding states. π and π^* overlap better with the two Al atoms in the twofold site, because their lobes are pointing outwards, directly at the two bridging Al. As a consequence, the Al- π and Al- π^* OPs are bigger on the twofold sites.



The C-C OP is also stronger in the twofold site than on top. In the on-top site, π has been depopulated by about $0.25 e^-$ (12.5%), while π^* has gained $1.69 e^-$ (84.5%). In the twofold site, π has been depopulated by $0.34 e^-$ (17.0%), while π^* is populated by $1.52 e^-$ (76.0%). Comparing these two sites, the C-C bond has lost more π character in the on-top site, thus the bond is weaker. The C=C (double bond) and C-C (single bond) overlap population in the free mole-

cule is around 1.30 and 0.74, respectively. So this C-C (OP = 0.752) bond on the surface resembles a single bond, even though the distance (1.45 Å), is between those of a single and double bond. There is obviously a lot of back-donation in this chemisorption, more than in usual metal-olefin interactions.

The total DOS curve with π and π^* projections in the twofold site on Al(100) is illustrated in Fig. 6. The respective orbital energies of a free, planar, undistorted ethylene are indicated by a bar at left. On both surfaces π has been pushed down about 1.3 eV, while π^* is pushed down around 0.5 eV. Also, judging from the integration curve, there are some states which are very high up, so there is a strong interaction between the surfaces and these two FMOs.

In conclusion, ethylene probably favors adsorption in the twofold sites on Al(111) and Al(100), through the overlap of its π and π^* orbitals with the Al $s + p_z$ bands. The substantial weakening of the C-C bond is primarily due to the population of the π^* level. The weakening of the C-C bond and the noncoplanarity of the ethylene is consistent with the trend in transition metal-olefin interactions in discrete molecules and on surfaces.

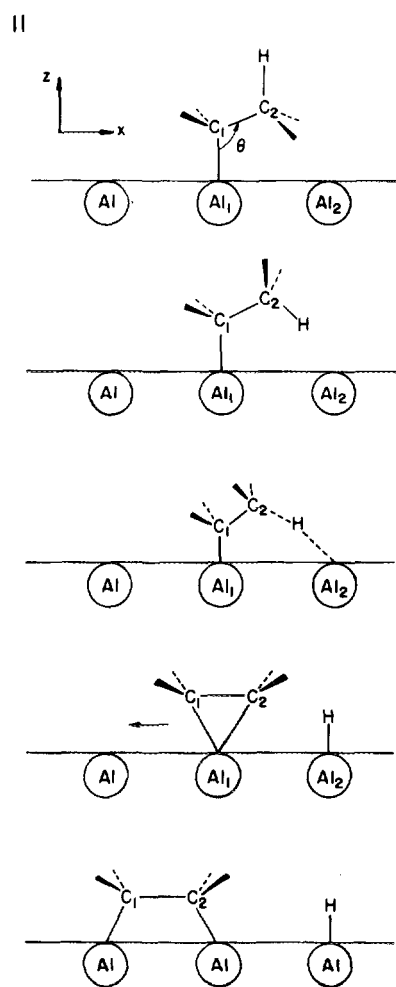
VII. SURFACE KINETICS

Now that all the favored sites for different adsorbates are determined, how exactly do these molecules move around on the surfaces? Let us review the binding energy of the above adsorbates in selected sites, Table VI. The Table gives relative energies, the reference site is the most favorable one of that species. The temperature of the experiment, ~ 500 K, would allow barriers of 2 to 3 eV to be overcome. From the numbers in the table, ethylene should be able to move around quite easily between on-top and twofold sites on the surfaces. C_2H_5 may also migrate, but less freely. H should probably not be moving around on the surface. We will use this knowledge to construct a reaction pathway for the reaction.

From the above information, ethylene should be the only species that is likely to move around on the surfaces. So we propose that after the Al is deposited on the surfaces, CH_3CH_2 adsorbs in the on-top site. Then the β -H interacts with another Al atom. While this C-H bond is breaking, an Al-H bond is forming. The C_2H_4 unit thus forms in the on-top site, then migrates to its preferred twofold site. Diagram 11 shows the pathway we presume. We have also studied other reaction pathways, but their activation energies are all higher than the β -elimination one, so only this one will be described in detail. This reaction has two steps then, with the β -elimination step being the rate-determining one. In Fig. 7, we present the calculated potential energy curve for this reaction for Al(111) and Al(100). In addition, some selected overlap populations for the Al(111) surface are shown (Those of Al(100) are similar except for $\text{C}_2\text{-H}$ OP, which then also shown in Fig. 7). The computed activation energy is 0.97 eV and 1.54 for Al(111) and Al(100), respectively. From the slopes of the two $\text{C}_2\text{-H}$ OP curves, the $\text{C}_2\text{-H}$ bond breaks faster on Al(111) than Al(100). This means the reaction on Al(111) has an earlier transition state than Al(100). The transition state on Al(111) comes indeed be-

TABLE V. Results of calculation for the chemisorption of C_2H_4 .

	On top		Twofold		Threefold/fourfold	
	111	100	111	100	111	100
BE (eV)	1.093	-0.468	3.400	0.277	-3.780	-6.676
Overlap populations						
C-C	0.663	0.663	0.765	0.752	0.690	0.779
Al-C	0.237	0.237	0.435	0.438	0.201	0.197
Al- σ	0.077	0.044	0.004	0.007	-0.005	-0.003
Al- π	0.103	0.091	0.132	0.141	0.030	0.053
Al s - π	0.035	0.008	0.042	0.039	-0.001	0.015
Al p_z - π	0.067	0.081	0.092	0.097	0.030	0.023
Al- π^*	0.057	0.085	0.298	0.291	0.180	0.138
Al s - π^*	-0.006	0.009	0.109	0.085	0.084	0.048
Al p_x - π^*	0.057	0.082	0.027	0.020	0.027	0.012
Al p_y - π^*	0.000	0.000	0.000	0.000	0.013	0.053
Al p_z - π^*	0.007	-0.002	0.162	0.187	0.056	0.023
FMO occupations						
π	1.814	1.751	1.737	1.664	1.776	1.517
π^*	1.804	1.694	1.571	1.518	1.680	1.624
Net charges for C_2H_4						
	-1.52	-1.36	-1.24	-1.12	-1.25	-0.96



fore that on Al(100) in Fig. 7.

The C_1 - Al_1 and C_2 -H and C-C OP decrease along the reaction pathway, while C_2 - Al_1 and Al_2 -H increase. These trends all fit into the basic reaction picture, except for the way the C-C overlap population varies. During this reaction, the C-C distance is decreasing from 1.54 to 1.45 Å. Why then is the C-C OP getting smaller? Figure 8 projects the DOS of the π and π^* orbitals vs the stretching of the C-C bond on the Al(111) surface.

The local C_2H_4 geometry has C_s symmetry, a mirror plane parallel to the xz plane, containing the β hydrogen. From the DOS plots, the HOMO of C_2H_4 [Fig. 8(a)] remains at almost the same energy along the reaction pathway.

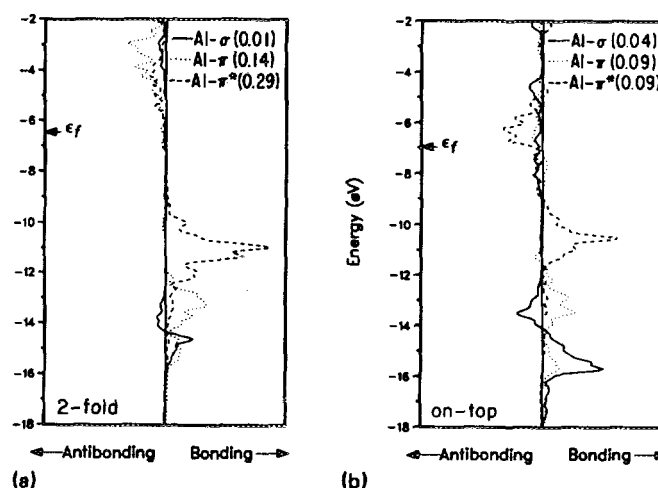


FIG. 5. (a) Al-C COOP curves in a FMO basis of adsorbed ethylene in the on-top site on Al(100). (b) Al-C COOP curves in a FMO basis of adsorbed ethylene in the twofold site on Al(100).

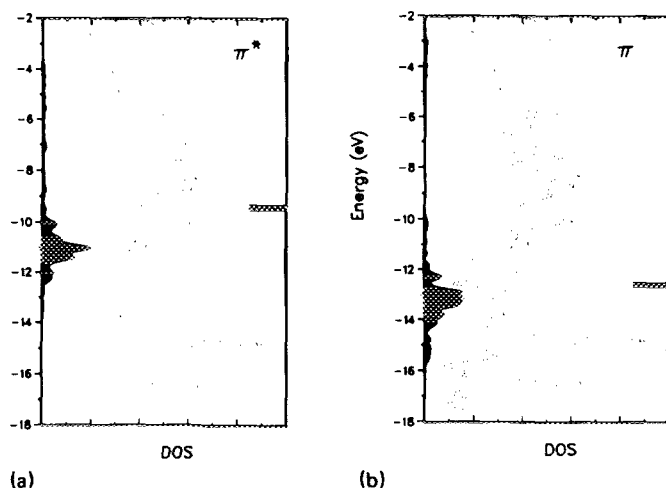


FIG. 6. (a) DOS of adsorbed ethylene at twofold site on Al(100) with projected π states ($2 \times$) and its integration curve (dotted line). The bar denotes the π MO energy of a free, coplanar, undistorted C_2H_4 before adsorption. (b) DOS of adsorbed ethylene at twofold site on Al(100) with projected π^* states ($2 \times$) and its integration curve (dotted line). The bar denotes the π^* MO energy of a free, coplanar, undistorted C_2H_4 before adsorption.

So this orbital could be thought of as evolving to π (HOMO of C_2H_4) [Fig. 8(e)]. Both the HOMO (which becomes π) and LUMO (becoming π^*) have a' symmetry so that they can mix. The evolution of these orbitals is drawn in Fig. 8. In addition, since the C_2H_5 is changing into a C_2H_4 , the π^* level, which originates at -1 eV, descends to -7 eV. The Fermi level of the whole system does not fluctuate much during this reaction. Thus when the π^* orbital is above the Fermi level, the C-C OP increases with decreasing C-C distance. When this π^* orbital comes below the Fermi level, then electrons will occupy it and the C-C OP is decreased. Basically the ethylene adsorbed on Al, as we discussed in a previous section, has a weak C-C bond due to extensive occupation of π^* .

A related orbital effect occurs for the Al_2-H and C_2-H OP. Figure 9 projects the H atom. One can see how this level (we call it $H\sigma$) moves down from 5 eV. Figure 10 shows the Al_2-H and C_2-H OP in one of the reaction steps, so one can see that $H\sigma$ actually is Al-H bonding and C-H antibonding below the Fermi energy. The sudden increase in Al-H and decrease in C-H bond strength is due to the occupation of this level.

TABLE VI. Energy barriers for migration pathway, in eV.

	On top		Twofold		Threefold/fourfold	
	111	100	111	100	111	100
H	0	0	3.78	1.41	5.16	4.95
CH_3	0	0	4.11	3.25	5.97	11.59
C_2H_5	0	0	4.34	3.36		
C_2H_4	2.31	0.75	0	0	7.18	6.95

J. Vac. Sci. Technol. A, Vol. 9, No. 3, May/June 1991

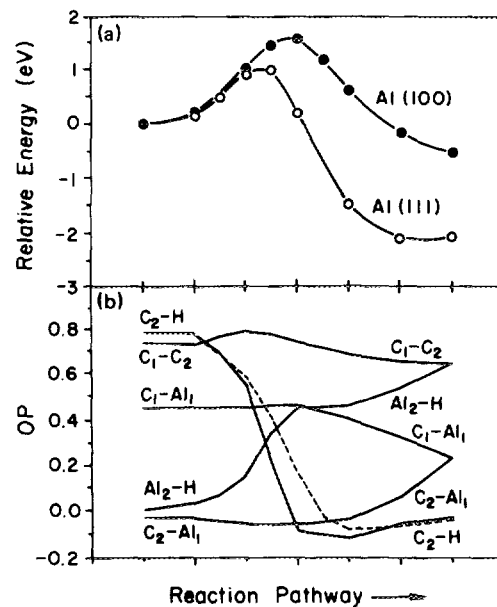


FIG. 7. (a) Calculated potential curves for Al(111) and Al(100). (b) Selected overlap populations for Al(111) and C_2-H OP (dotted line) for Al(100).

We find that the reaction mechanism for both surfaces is very similar. It seems that an orientation factor is not governing the selectivity of these two surfaces. This is not surprising. If the reaction occurs along the line between the on-top site and twofold site, as we have assumed, then both of the surfaces have the same local geometry. The calculated

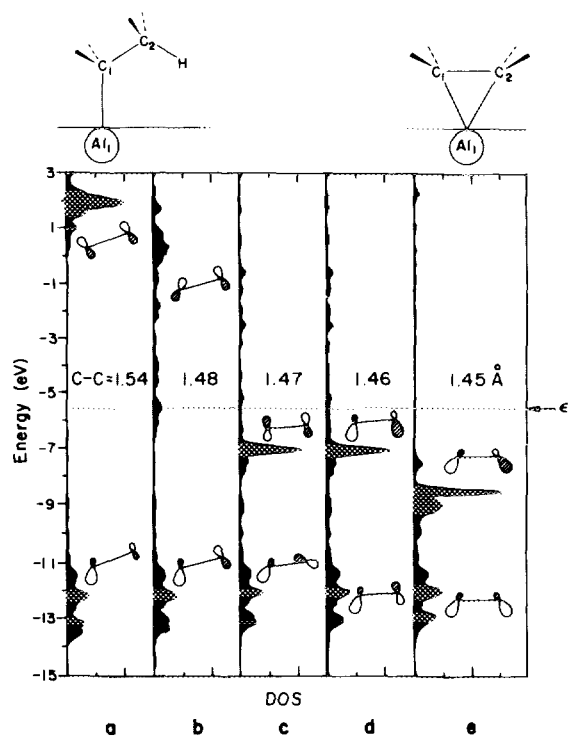


FIG. 8. The evolution of ethylene π and π^* orbitals along the β -elimination pathway on Al(111). The C-C bond length is specified.

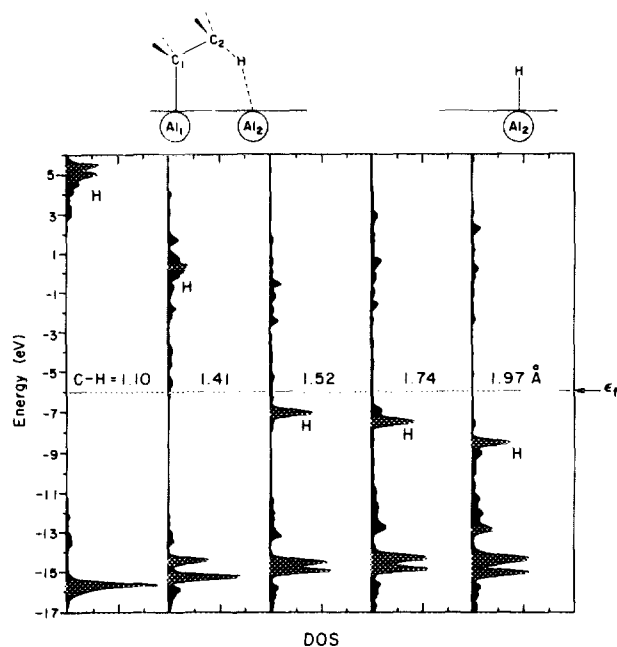


FIG. 9. The evolution of the H states along the β -elimination pathway on Al(111). The C-H distance is marked.

activation energy is indeed smaller for the Al(111) case. This is perhaps due to better charge transfer between the adsorbates and the Al(111) surface. During the rate-determining stage, $H\sigma$ comes down in energy, as shown above. If there is more electron transfer to this orbital, the C-H bond will break easily, enhancing the β -elimination reaction. Note that the slope of the C-H overlap population curve is bigger in Al(111) than in Al(100). So this agrees with a

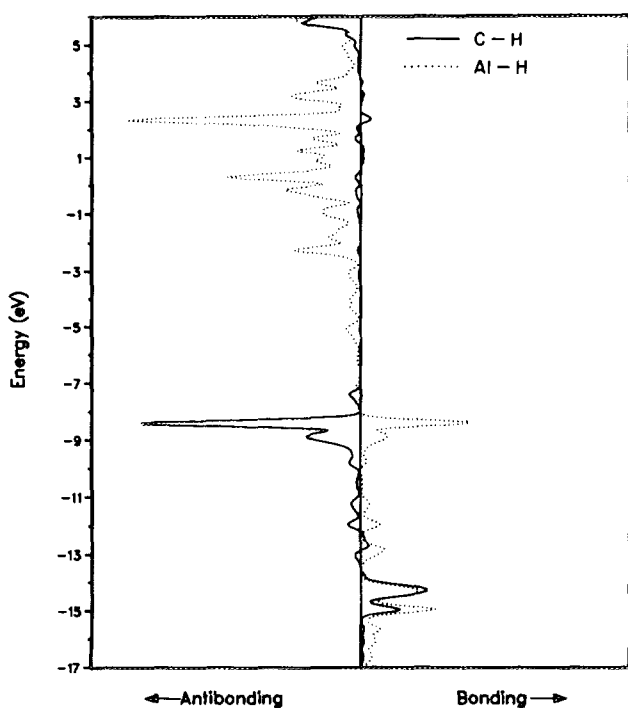


FIG. 10. Al-H and C-H COOP curves in one of the steps (at C-H and Al-H distances of 1.74 and 1.93 Å, respectively) along the β -elimination pathway on Al(111).

J. Vac. Sci. Technol. A, Vol. 9, No. 3, May/June 1991

TABLE VII. Extended Hückel parameters.

Atom	Orbital	H_n (eV)	ζ_1
Al	2s	-12.6	1.370
	2p	-7.0	1.370
C	2s	-18.6	1.750
	2p	-14.0	1.300
H	1s	-40.0	2.425

sharper change of bond strength because of greater electron transfer.

VIII. SUMMARY

The analyses of the chemisorption of four different species, which are related to the Al CVD reaction, have been studied. Basically, the adsorbate-surface bonding is characterized by orbital interactions with the Al $s + p_z$ orbitals. Hydrogen, methyl, and ethyl occupy the on-top site through a σ -type interaction, using their HOMOs. Ethylene, by virtue of a di- σ bonded interaction through its π and π^* orbitals with the surface, sits in the twofold bridging site. The rate-determining step in the Al CVD reaction is probably the β -H elimination mechanism. Better charge transfer may be a reason why the reaction rate is faster on Al(111) than on Al(100).

ACKNOWLEDGMENTS

Our work was supported by the Office of Naval Research. We are grateful to Jane Jorgensen and Elisabeth Fields for the drawings, and to Brian Bent for discussion of this problem.

APPENDIX

The tight-binding extended Hückel method³⁸ was used for all the calculations. Parameters used are listed in Table VII.

We defined the binding energy (BE) as $E(\text{slab}) + E(\text{adsorbate}) - E(\text{composite system})$.

The density of states of the bulk Al is computed by an extended Hückel calculation using 110 k points. Two different sets of 16 k points³⁹ were used in Al(111) and Al(100) surface calculations.

¹ S. M. Sze, *Semiconductor Devices: Physics and Technology* (Wiley, New York, 1985), Chap. 9, and references therein.

² K. Ziegler, K. Nagel, and W. Pfohl, *Justus Liebigs Ann. Chem.* **629**, 210 (1960).

³ B. E. Bent, R. G. Nuzzo, and L. H. Dubois, *J. Am. Chem. Soc.* **111**, 1634 (1989). *J. Vac. Sci. Technol. A* **6**, 1920 (1988). *Mat. Res. Soc. Symp. Proc.* **101**, 177 (1988).

⁴ G. S. Higashi, K. Raghavachari, and M. L. Steigerwald, *J. Vac. Sci. Technol. B* **8**, 103 (1990); G. S. Higashi, *Appl. Surf. Sci.* **43**, 6 (1989).

⁵ For a description of the methodology and the use of these indices in tracing down orbital interactions, see R. Hoffmann, in *Solids and Surfaces: A Chemist's View in Bonding in Extended Structures* (VCH, New York, 1988).

⁶ G. E. Coates and K. Wade, *Organometallic Compounds, Volume 1: The Main Group Elements* (Methuen, London, 1967), p 320.

⁷ J.-Y. Saillard and R. Hoffmann, *J. Am. Chem. Soc.* **106**, 2006 (1984). A. W. E. Chan and R. Hoffmann, *J. Chem. Phys.* **92**, 699 (1990).

- ⁸ C. Kittel, *Introduction to Solid State Physics* (Wiley, New York, 1986).
- ⁹ C. J. Ballhausen and H. B. Gray, *Molecular Orbital Theory* (Benjamin, New York, 1965); S. P. McGlynn, L. G. Vanquickenborne, M. K. Kinoshita, and D. G. Carroll, *Introduction to Applied Quantum Chemistry* (Holt, Rinehart and Winston, New York, 1972), p 139, Appendix D.
- ¹⁰ K. Jacobi, C. Astaldi, P. Geng, and M. Bertolo, *Surf. Sci.* **223**, 569 (1989).
- ¹¹ G. D. Waddill and L. L. Kesmodel, *Surf. Sci.* **182**, L248 (1987).
- ¹² G. V. Hansson and S. A. Flodström, *Phys. Rev. B* **18**, 1562 (1978).
- ¹³ P. O. Gartland and B. J. Slagsvold, *Solid State Commun.* **25**, 489 (1978).
- ¹⁴ K. Christmann, *Surf. Sci. Rep.* **9**, 1–3 (1988) and references therein.
- ¹⁵ See, for example, M. A. Van Hove and S. Y. Tong, *Surface Crystallography by LEED* (Springer Series in Chemical Physics, Springer, Berlin, 1979), Vol. 2.
- ¹⁶ See, for example, *Vibrational Spectroscopy of Adsorbates*, edited by R. F. Wills (Springer Series in Chemical Physics, Springer, Berlin, 1980), Vol. 15, p. 23ff.
- ¹⁷ J. Paul, *Phys. Rev. B* **37**, 6164 (1988).
- ¹⁸ H. Hjelmberg, *Surf. Sci.* **81**, 539 (1979); O. Gnnarson, H. Hjelmberg, and B. I. Lundqvist, *Phys. Rev. Lett.* **37**, 292 (1976).
- ¹⁹ E. P. Smirnov, *Theor. Exp. Chem.* **19**, 324 (1983).
- ²⁰ Y. Xie and H. F. Schaefer, *J. Am. Chem. Soc.* **112**, 5393 (1990).
- ²¹ A. Almennigen, G. Gundersen, T. Haugen, and A. Harland, *Acta Chem. Scand.* **26**, 3928 (1972).
- ²² J. Li, B. Schiøtt, R. Hoffmann, and D. M. Proserpio, *J. Phys. Chem.* **94**, 1554 (1990).
- ²³ A. Almennigen, S. Halvorsen, and A. Haaland, *Acta Chem. Scand.* **25**, 1937 (1971).
- ²⁴ J. W. Moore, D. A. Sanders, P. A. Scher, M. D. Glick, and J. P. Oliver, *J. Am. Chem. Soc.* **93**, 1035 (1971).
- ²⁵ From a crystallographic search using the Cambridge Data Base.
- ²⁶ C. Zheng, Y. Apeloig, and R. Hoffmann, *J. Am. Chem. Soc.* **110**, 749 (1988).
- ²⁷ J. Schüle, P. Siegbahn, and U. Wahlgren, *J. Chem. Phys.* **89**, 6982 (1988).
- ²⁸ Q. P. Yang and S. T. Ceyer, *J. Vac. Sci. Technol. A* **6**, 851 (1988).
- ²⁹ M. R. Albert and J. T. Yates, in *The Surface Scientist's Guide to Organometallic Chemistry* (American Chemical Society, Washington, DC, 1987).
- ³⁰ P. H. Kasai and D. J. McLeod, *J. Am. Chem. Soc.* **97**, 5609 (1975).
- ³¹ Y. Xie, B. F. Yates, Y. Yamaguchi, and H. F. Schaefer, *J. Am. Chem. Soc.* **111**, 6163 (1989).
- ³² J. Gao and M. Karplus, *Chem. Phys. Lett.* **169**, 410 (1990).
- ³³ J. L. Duncan and I. J. Wright, *J. Mole. Spectrosc.* **42**, 463 (1972). N. Sheppard, *Annu. Rev. Phys. Chem.* **39**, 589 (1988) and references therein.
- ³⁴ H. Ibach and S. Lehwald, *J. Vac. Sci. Technol.* **15**, 407 (1978).
- ³⁵ C. Nyberg, C. G. Tengstal, S. Andersson, and M. W. Holmes, *Chem. Phys. Lett.* **87**, 87 (1987).
- ³⁶ T. H. Felter and W. H. Weinberg, *Surf. Sci.* **103**, 265 (1981).
- ³⁷ H. Ibach, H. Hopster, and B. Sexton, *Appl. Surf. Sci.* **1**, 1 (1977).
- ³⁸ R. Hoffmann and W. N. Lipscomb, *J. Chem. Phys.* **36**, 2179 (1962); **37**, 2872 (1962). R. Hoffmann, *ibid.* **39**, 1397 (1963).
- ³⁹ R. Ramirez and M. C. Böhm, *Int. J. Quantum Chem.* **34**, 571 (1988).